

Shaping of Alginate–Silica Hybrid Materials into Microspheres through Vibrating-Nozzle Technology and Their Use for the Recovery of Neodymium from Aqueous Solutions

Joris Roosen,^{†,‡} Judith Pype,^{†,§} Koen Binnemans,^{*,‡} and Steven Mullens[†]

[†]Sustainable Materials Management, Flemish Institute for Technological Research (VITO), Boeretang 200, 2400 Mol, Belgium

[‡]Department of Chemistry, KU Leuven, Celestijnenlaan 200F, P.O. Box 2404, 3001 Heverlee, Belgium

[§]Department of Chemistry, University of Antwerp, Universiteitsplein 1, 2610 Wilrijk, Belgium

S Supporting Information

ABSTRACT: The vibrating-nozzle technology is very interesting to very easily and very rapidly produce industrial amounts of functional microspheres. The technology was used to make hybrid alginate–silica microspheres by droplet coagulation. The microspheres were formed starting from suspensions of sodium alginate, and coagulation occurred in an aqueous solution of calcium ions. To enhance the mechanical properties of the alginate raw material, it was combined with two different silica sources: tetramethyl orthosilicate (TMOS) and commercial silica powder. The two different batches of alginate–silica microspheres were fully compared with regard to their morphology, composition, shrinking behavior, and stability in acidic conditions. It was shown that the incorporation of an inorganic matrix resulted in a material with a better stabilized porous structure and a higher resistance in an acidic environment. Both are important when functional particles are designed to be used for adsorption of metal ions, either as a stirred suspension or as a stationary phase in a chromatographic column. A study of the adsorption performance was conducted in batch mode for neodymium(III), a representative element for the group of critical rare-earth elements. The effect of stripping (desorption) on the adsorption performance and reusability was also investigated. The functional alginate–silica microspheres show a sustainable character.

■ INTRODUCTION

Biopolymers, such as chitosan and alginate, are very useful for the removal of metal ions from aqueous solutions by adsorption, both in the context of wastewater treatment to purify waste streams from toxic (heavy) metal ions and in the context of wastewater valorization to recover valuable metal ions from these secondary resources.^{1–9} The great interest of researchers in these materials arises from their advantages. They are bioavailable and thus characterized by a quasi-unlimited and low-cost supply, they show a high adsorption capacity, they are reusable, etc.^{2,3,7,10} On the other hand, biopolymers have some drawbacks. They are generally nonporous, show high swelling behavior, and have an elastic character. These shortcomings can be overcome by incorporation of a silica source, in order to build an inorganic matrix in the structure and hence create functional organic–inorganic materials with superior characteristics.^{11–19} These hybrid materials can then be applied as stationary phases in large column chromatography setups. However, when it is intended to use these materials for applications on a large industrial scale, the physical appearance of the materials becomes more important. The shaping of high-performance materials into spheres enhances the ease of use and storage in comparison with powders.²⁰ Also, a smooth eluent flow through the column can be guaranteed without clogging problems because the porosity is generally included in these spheres during their formation.²⁰ Moreover, the adsorption performance of the column material could be improved by rational design and synthesis. Indeed, expansion of the biopolymer network improves access to internal sorption

sites, which could enhance the adsorption capacity of the adsorbent materials and the selectivity for the metals of interest. Here, the shaping of alginate–silica hybrid materials into microspheres was done by the principle of microencapsulation. Microencapsulation is the general term for the coating of small solid particles, liquid droplets, or gas bubbles with a film of shell material.²¹ The capsules thus produced are usually from the micrometer to millimeter range and are therefore called microspheres.²² Microsphere formation mainly finds application in the fields of pharmaceuticals,^{23,24} biotechnology,^{25,26} and food technology.^{27,28} However, microspheres can also be applied in the field of hydrometallurgy because adsorption is believed to be an efficient and environmentally friendly technique for the recovery and separation of metal ions from aqueous streams, certainly when taking advantage of biosorbents like chitosan or alginate.^{1,8,9,29} Different technologies exist for the formation of microspheres, such as spray drying,³⁰ fluid bed coating,³¹ coacervation,³² spheronization,³³ annular jet,³⁴ etc. For practical use in hydrometallurgical applications, the authors consider the vibrating-nozzle technology as the best option for the creation of large batches of functional microspheres. The vibrating-nozzle technology offers the capability of producing industrial-scale quantities of spherical and especially monodisperse particles in short production

Received: September 18, 2015

Revised: November 26, 2015

Accepted: November 30, 2015

Published: November 30, 2015

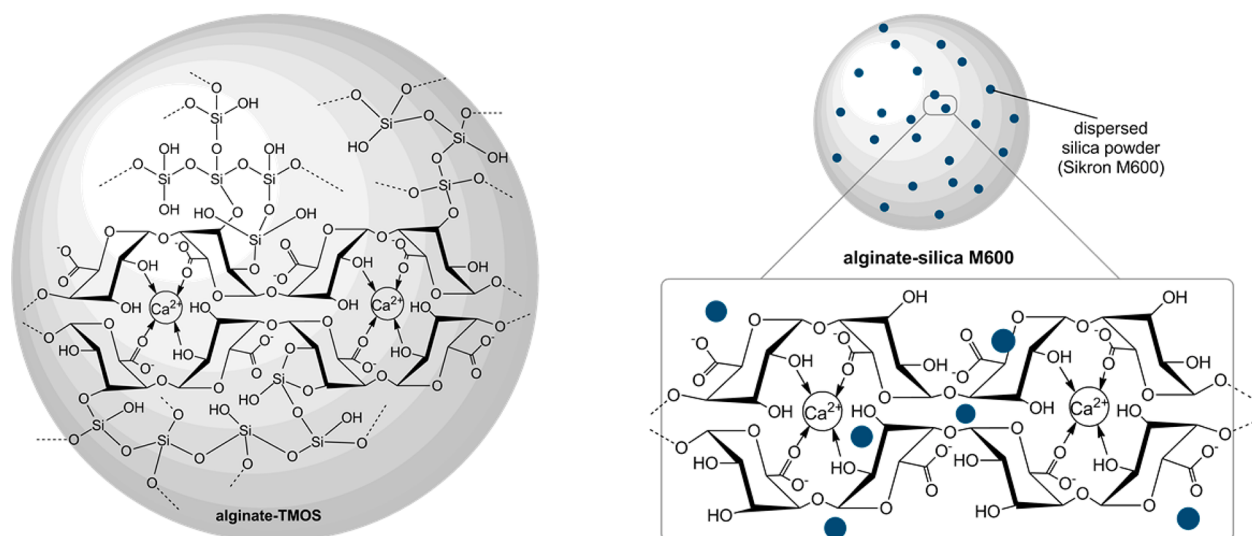


Figure 1. Schematic structure of alginate microspheres, interpenetrated with in situ polymerized silica networks by soaking in a TMOS solution (left) and incorporated with dispersed silica powder – Sikron M600 (right).

times.²⁰ By making use of the vibrating-nozzle technology, the process is considered to have the following advantages: (1) easy scale-up from laboratory scale to pilot scale; (2) formation of microspheres with a monomodal and narrow size distribution; (3) possibility of flexibly adjusting the diameter range by variation of the nozzle size, suspension viscosity, frequency, and pressure; (4) a small ecological footprint of the setup and limited energy consumption.

In this article, two approaches for the creation of hybrid alginate–silica microspheres were tried and compared (Figure 1). One method consists of the addition of a fine-grained silica powder to the alginate suspension before dripping. In this way, a composite material is obtained (alginate–silica M600) with easily tunable characteristics by the choice of the proper silica powder. The other method consists of inducing in situ silica polymerization by soaking pure alginate microspheres in tetramethyl orthosilicate (TMOS).³⁵ The latter sol–gel procedure comprises hydrolysis reactions to replace methoxide groups with hydroxyl groups, resulting in hydrophilic silanol entities, which subsequently undergo condensation reactions to form siloxane bonds within the microspheres.³⁶ Because hydroxyl groups of silanol and alginate can coreact, a so-called interpenetrating-network (IPN) material with enhanced rigidity is expected (alginate–TMOS).

The naming of the particles in this work refers to the origin of silica incorporation (silica M600 and TMOS). A full characterization was done for both batches, with respect to their morphology, composition, shrinking behavior and stability in acidic environment. A clear and full comparison of the resulting characteristics of the alginate microspheres for both approaches of silica incorporation has not been described before. Also the adsorption performance of the hybrid materials was investigated for neodymium(III) (Nd^{III}), considered as a model element for the group of rare-earth elements (REEs). Much research is going on to achieve sustainable valorization schemes for waste streams, like industrial process residues, containing these REEs.³⁷ Finally, the effect of stripping on the adsorption performance and reusability was investigated in order to be able to evaluate the sustainable character of the synthesized materials.

EXPERIMENTAL SECTION

Chemicals. Scogin LV (low viscosity) sodium alginate was kindly supplied by FMC BioPolymer (Philadelphia, PA). The mannuronate–guluronate (M:G) ratio was 3:2 (60% M and 40% G). The viscosity specification range was between 50 and 70 mPa·s (1 wt % solution). Tetramethyl orthosilicate (TMOS), $\geq 98.0\%$ purity, was purchased from Fluka Chemie GmbH (Buchs, Switzerland). Quartz silica powder Sikron M600 was supplied by SCR-Sibelco NV (Dessel, Belgium). It had a median (d_{50}) diameter of 3 μm and a specific surface area of 4.2 m^2/g . Hydrochloric acid, 30%, for analysis (Emsure), hydrated calcium chloride for elemental analysis, and Uvasol ethanol for spectroscopy were purchased from Merck KGaA (Darmstadt, Germany). Ethanol 96% AnalaR NORMAPUR and Ph. Eur. Ethanol absolute were purchased from VWR Chemicals BDH Prolabo (Leuven, Belgium). $\text{Nd}(\text{NO}_3)_3 \cdot 6\text{H}_2\text{O}$ (99.9%) was supplied by Alfa Aesar (Ward Hill, MA). Chemicals were used without further purification. Water (Milli-Q) was always of ultrapure quality.

Equipment and Analysis. The formation of alginate–silica microspheres was done by means of the Microspherisator M from Brace GmbH (Karlstein am Main, Germany). This small pilot-scale device has a capacity of up to 10 L/h. A schematic presentation of the experimental setup is shown in Figure 2.

A HAAKE MARS Modular Advanced Rheometer System (Thermo Electron Corp.) with a temperature controlling unit was used to perform viscosity measurements. Samples were measured in a coaxial cylinder with a Z41Ti spindle, at 25 °C. Shear rates were varied from 0.1 to 1000 s^{-1} . Microscopic pictures for particle size analysis were taken with a Zeiss SteREO Discovery.V12 microscope, equipped with a Plan Apo S 1.0x FWD 60 mm objective, a digital Axiocam MRc camera, and a KL2500 LCD light source. Particle size analysis was carried out on a minimum of 100 microspheres with the AxioVision 4 Module Particle Analyzer software. Fourier transform infrared (FTIR) spectra were recorded on a Bruker Vertex 70 spectrometer (Bruker Optics). Air-dried samples were crushed and examined as such using a Platinum ATR single reflection diamond attenuated total reflection accessory. Carbon, hydrogen, and nitrogen (CHN) elemental analyses were obtained with a TruSpec CHN element analyzer (LECO,

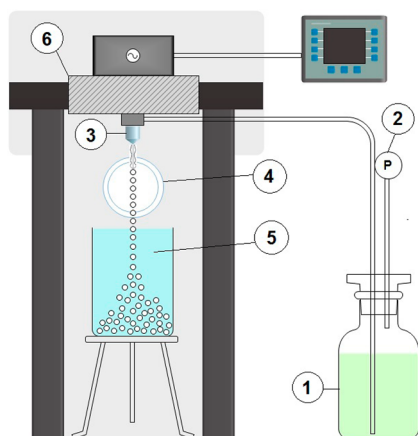


Figure 2. Schematic presentation of the experimental vibrating-nozzle setup: 1, feed vessel; 2, pressure pump; 3, vibrating nozzle; 4, stroboscopic light; 5, coagulation bath; 6, pulsation chamber.

St Joseph, MI). Thermogravimetric analyses (TGA) were performed using a Netzsch-Gerätebau STA 449 C Jupiter thermomicrobalance. Samples were analyzed from ambient temperature to 1000 °C under flowing air at a heating rate of 5 °C/min. Some of the particles were dried by supercritical CO₂, in order to remove all liquid in a controlled way, without capillary forces damaging the raw structure. This was done by using a BAL-TEC CPD 030 Critical Point Dryer. Prior to drying, the water in the microspheres was fully replaced by ethanol because water and liquid CO₂ are not miscible. This was done by soaking the microspheres in ethanol of gradually increasing purity: a first time in 96 vol % ethanol, then in absolute ethanol, and finally in ethanol Uvasol. The drying procedure was then started by replacing ethanol with liquid CO₂ in the microspheres. This was done by refreshing the medium in the drying chamber with pure liquid CO₂, rinsing, and draining (five times). To make liquid CO₂ supercritical, the temperature and pressure in the chamber were increased above the critical point of CO₂, which is at 31 °C and 73.8 bar. Then by gentle release of supercritical CO₂, the pressure of the chamber decreased again to atmospheric pressure, leaving behind the dried product. The surface of the intact supercritical CO₂ dried microspheres was observed using a Nova Nano-sem450 cold field-emission scanning electron microscope (FEI, Hillsboro, OR) at an acceleration voltage of 5 keV. To avoid charging under the electron beam during scanning electron microscopy (SEM), all samples were coated with a thin Pt(80)/Pd(20) layer (~1.5 nm), using a Cressington 208 HR high-resolution sputter coater. Another part of the microspheres was freeze-dried with a Heto Power Dry LL3000 Freeze Dryer with a HSC500 temperature controller. The microspheres were frozen in liquid nitrogen prior to sublimation of the water in the microspheres under vacuum. The specific surface areas of the freeze-dried adsorbents were determined with a Quantachrome Autosorb-iQ automated gas sorption analyzer. Samples were outgassed under an inert helium purge at room temperature. The specific surface areas were determined with the Brunauer–Emmett–Teller (BET) method from N₂ adsorption and desorption isotherms at liquid-nitrogen temperature. Metal-ion concentrations were determined by total-reflection X-ray fluorescence (TXRF) on a Bruker S2 Picofox TXRF spectrometer. To perform the sample preparation for TXRF measurement, an aqueous metal solution (500 μL) was added

in an Eppendorf tube with a 1000 mg/L Merck gallium standard solution (100 μL) and diluted with Milli-Q water (400 μL). A small amount of the sample (7.5 μL) was put on a quartz disk, precoated with a hydrophobic silicone solution (10 μL), and dried in an oven at 60 °C for 30 min. Samples were then measured for 300 s. The investigation of silicon leaching required the use of polypropylene disks, instead of quartz carriers.

Synthesis. Alginate–TMOS. First, a suspension (1 L) was made by mixing sodium alginate (3 wt %) in Milli-Q water. The suspension was stirred overnight to ensure full homogenization. A flow was initiated by putting the liquid feed under pressure. With a stroboscopic light that flashes in phase with the nozzle vibration, the breakup of the jet could be visualized. This is important to optimize the parameters of the process, which is necessary for a good breakup of the droplets. After this, the microspheres were caught in a coagulation bath (1 L), being a solution of CaCl₂ [2.5% (w/v)]. The dripping height was kept constant on the position of the first free droplet of the interrupted jet. The spheres (500 mL) were rinsed three times with Milli-Q water and stored for 24 h. Next, half of the spheres (250 mL) was carefully transferred to a 1:1 mixture of TMOS in ethanol (500 mL), in which they matured overnight. The spheres were isolated, stirred for 2 h in Milli-Q water, sieved, and then soaked in a 1:1 mixture of glycerol in Milli-Q water (500 mL) for 4 h. Finally, the hybridized microspheres were rinsed three times with Milli-Q water and then stored in Milli-Q water.

Alginate–Silica M600. A similar method was used to prepare alginate–silica M600 microspheres. Prior to the coagulation process, Sikron silica M600 powder [2% (w/v)] was added to the sodium alginate suspension [3% (w/v)]. After stirring, potential agglomerates were filtered off by a 100 μm sieve. Because of a different composition of the suspension, the instrument parameters for the vibrational droplet coagulation were different (Table S2). The spheres (500 mL) were rinsed and stored in Milli-Q water.

Adsorption Experiments. Prior to the adsorption experiments, the stability in an acidic environment was investigated. Wet microspheres (500 ± 5 mg) were added to acidified solutions (10.0 mL), with concentrations of HCl varying from 0.00 to 5.00 M. The solutions were stirred at 300 rpm for 4 h, after which the aqueous phase was decanted for analysis with TXRF.

Batch adsorption experiments were conducted in aqueous solutions to investigate the adsorption performance of the microspheres. A stock solution of Nd^{III} was prepared ($c_{\text{aq}} = 10.00 \pm 0.10$ mM). Wet microspheres (500 ± 5 mg) were added to a properly diluted solution of Nd^{III} (10.0 mL) and magnetically stirred at 300 rpm and room temperature. At equilibrium (within 4 h), the aqueous phase was decanted for analysis with TXRF. The amount of metal ions adsorbed was then quantified using the following formula:

$$q_e = \frac{(c_i - c_e)V}{m_{\text{ads}}} \quad (1)$$

In this formula, q_e is the amount of adsorbed metal ions at equilibrium (mmol/g adsorbent), c_i is the initial metal-ion concentration in aqueous solution (mmol/L), c_e is the equilibrium metal-ion concentration in aqueous solution (mmol/L), V is the volume of the solution (L), and m_{ads} is the mass of the adsorbent (g). Adsorption was investigated as a

function of the pH, adjusted by adding proper amounts of HCl (1.0 M) or NaOH (0.1 M) to decrease or increase the pH, respectively. Wet spheres were used for reasons of convenience and because of the fact that water-saturated spheres would also be used in column applications. Adsorption amounts were recalculated to dry mass by correcting for the water content (*vide infra*). This was done to simplify comparison with similar systems in the literature.^{8,38–42}

The water content was determined by weighing an amount of wet spheres, then increasing the temperature in a TGA device (10 °C/min), and considering the residual (dry) mass after a stabilization period of 30 min at 105 °C (Table 1).

Reusability Study. Studies on the reusability of the microspheres were performed to investigate the adsorption efficiency for consecutive adsorption/desorption cycles. Adsorption was done by adding wet microspheres (500 ± 5 mg) in plastic centrifuge tubes containing aqueous Nd^{III} solutions ($c_{\text{aq}} = 1.00 \pm 0.01$ mM). After 4 h of shaking at 1000 rpm, the aqueous solutions were separated by decantation for analysis with TXRF to determine the adsorption amount. Then, the particles were washed with Milli-Q water (10.0 mL) to remove Nd^{III} ions that were not coordinated. Subsequently, desorption was achieved by stripping the particles with a solution of HCl (0.5 M, 10.0 mL). The particles were shaken at 1000 rpm for 1 h. The stripping solution was separated by decantation prior to analysis with TXRF. The stripping percentage is defined as

$$\% \text{ stripping} = \frac{n_{\text{Nd,stripping solution}}}{n_{\text{Nd,adsorbed}}} \times 100\% \quad (2)$$

with $n_{\text{Nd,stripping solution}}$ the molar amount of Nd^{III} in the HCl solution and $n_{\text{Nd,adsorbed}}$ the molar amount of Nd^{III} that was adsorbed on the sorbents.

A 0.5 M HCl concentration was used in the reusability experiments in order to ensure full stripping. Three washing steps with Milli-Q water were performed before starting a new adsorption/desorption cycle, in order to get the particles pH-neutral. The experiment was done in triplicate to minimize the experimental error.

RESULTS AND DISCUSSION

Because of previous experience with functionalized chitosan, the authors initially intended to create microspheres starting from a chitosan material.^{43,44} Chitosan is a well-known material in the context of microencapsulation because of its gel-forming behavior.^{13,14,45–49} In chitosan, the formation of a gel is based on the principle of pH inversion when an acidic suspension is dropped into an alkaline coagulation bath. Unfortunately, the thus-formed spheres lacked any mechanical stability to resist the high impacts with the surface of the coagulation solution when dripped under high pressure with the Microspherisator. Several approaches were tried (addition of additives, reduction of the surface tension of the coagulation solution, increase of the viscosity and/or the density of the suspension, variation of the pH, etc.), but nothing could prevent deformations of the fragile spheres formed by breakup of the annular stream by the vibrating nozzle. Another biopolymer, very comparable to chitosan, is alginate. Both have the same advantages, such as their bioavailability, quasi-unlimited and cheap supply, reusability, and high adsorption capacity for metal ions. However, alginate microspheres show higher mechanical strength than chitosan microspheres.⁵⁰ With alginate, coagulation is based on the ionotropic gelation of alginate drops in a solution of

multivalent cations.⁵¹ Usually calcium chloride is used for coagulation. Note in Figure 1 the so-called egg-box structure that results from the specific coordination of calcium ions in alginate guluronate blocks. The formation of junction zones involves dimerization of alginate polymer chains, hence giving rise to a very stable structure.⁵² Preliminary tests showed that sodium alginate was more suitable as a starting material for the shaping of high-performance sorbent microspheres by means of vibrating-nozzle technology. Organic–inorganic hybrid materials were produced to improve the characteristics of the coagulated microspheres. Two different hybridization approaches were compared regarding their performance. In one batch, pure alginate microspheres were soaked in a TMOS–ethanol solution to obtain an IPN material. In another batch, silica powder (Sikron M600) was added to the alginate suspension, prior to coagulation, to obtain a composite material. Both approaches have their benefits and drawbacks, as will be discussed in the text. Note that the silica matrix is not necessary for the shaping but is only incorporated to improve the stability of the thus-formed microspheres, their acid resistance, the resulting rigidity, the column flow properties, etc.

Viscosity Study. The viscosity of the suspension has to be more or less between 50 and 800 mPa·s to ensure that the vibrational droplet coagulation process proceeds successfully. Therefore, viscosity profiles were measured for suspensions of 1.0, 2.0, 3.0 and 4.0% (w/v) of sodium alginate (Figure 3).

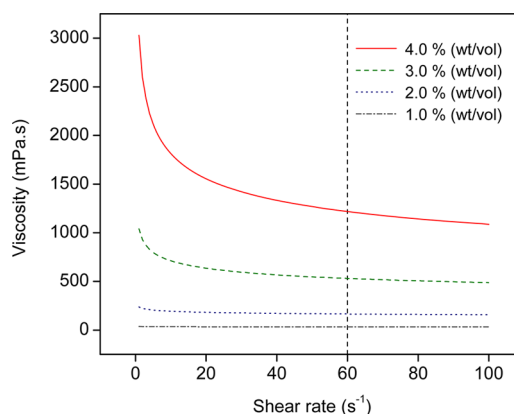


Figure 3. Viscosity profiles measured at 25 °C as a function of the shear rate for aqueous suspensions with varying sodium alginate concentrations. The vertical dashed line at 60 s⁻¹ indicates the shear rate that is comparable with the circumstances in the nozzle during vibrational droplet coagulation.

In Figure 3, the experimental data were fitted with the Ostwald–de Waele (power-law) model, which is based on the equation⁵³

$$\mu = K\dot{\gamma}^{n-1} \quad (3)$$

In this equation, μ (Pa·s) is the apparent viscosity, $\dot{\gamma}$ (s⁻¹) is the shear rate, and K (Pa·sⁿ) and n (dimensionless) are the flow consistency and flow behavior indices, respectively. The empirical parameters derived from fitting the experimental data with the Ostwald–de Waele model give information about the flow behavior and consistency of the suspension (Table S1).

Suspensions encounter certain forces during their processing as a consequence of the feed pressure, the vibrating nozzle, etc. On the basis of the viscosity values at the shear rate comparable

with the circumstances during the vibrational droplet coagulation process ($\dot{\gamma} = 60 \text{ s}^{-1}$; vertical dashed line in Figure 3), a 3.0% (w/v) sodium alginate suspension was considered to be the best choice for our process.

Two different types of silica sources were tested in order to compare the combined properties of the resulting alginate–silica microspheres: (1) TMOS, to induce in situ silica polymerization reactions, which results in an IPN material constituted of alginate and silicate interacting on a molecular level; (2) silica powder, to obtain a composite (multiphase) material in which the silica (filler) phase is dispersed in the alginate (matrix) phase. Alkoxysilanes such as tetramethoxysilane (TMOS) and tetraethoxysilane (TEOS) are common silicon-containing precursors for silica formation in materials for technological applications.³⁶ By soaking of the alginate microspheres in a TMOS solution, the aim was to induce in situ silica polymerization reactions, in order to obtain an IPN material (alginate–TMOS). Those materials possess a strong hybrid character and are thus expected to be very stable. In aqueous solutions, TMOS hydrolyzes, which results in the formation of silanol entities. In the subsequent condensation reactions, the formed silanol groups react in order to produce siloxane bonds.⁵⁴ Silica polymerization is usually catalyzed in an acidic or alkaline environment. However, it was observed that the silica polymerization proceeded well in a neutral environment because of the presence of –OH groups on the alginate moieties, which act as nucleation sites at which polymerization could start.³⁵ The major advantage of this approach is that chemical interactions and linkages occur between both materials (alginate and silicate), which results in a naturally cross-linked, IPN material. The other approach to incorporating an inorganic matrix in the organic microspheres was by adding silica powder to the alginate suspension. To decide which type of silica was the most suitable, we had to compromise between several characteristics. On the one hand, the particle size should be sufficiently small in order to have a high specific surface area. On the other hand, the specific surface area cannot be too high because this would increase the viscosity of the alginate suspension drastically, which would make it impossible to drip. Moreover, the powder must have sufficient density to keep dripped microspheres from floating on the surface of the coagulation bath and colliding with incoming spheres. Despite having large surface areas (50–600 m^2/g), fumed silica sources were therefore considered unsuitable as additives in the alginate suspension because the resulting suspensions have too high viscosities and too low densities (0.16–0.19 g/cm^3). Sikron silica sands are micrometer-sized and, with a density of 2.65 g/cm^3 , sufficiently heavy to make the formed microspheres sink to the bottom. Within the Sikron series, the Sikron M600 silica type was chosen because it has the highest specific surface area (4.20 m^2/g), which is due to its small (and well-controlled) particle-size distribution, with a d_{90} value of 9 μm and a d_{10} value of 2 μm . A d_{90} particle-size value is defined as the value where 90% of the population is smaller than this size and thus gives an idea about the size of the largest particles. Analogously, the d_{10} particle-size value represents the size where only 10% of the microspheres resides below. The eventual application of the functional particles determines the choice of the silica powder. Hence, an important advantage of adding silica powder over TMOS is that the characteristics of the resulting microspheres can be easily tuned by choosing the proper silica type.

The addition of 2.0% (w/v) silica M600 powder to the pure 3.0% (wt/vol) sodium alginate suspension led to an increase in the viscosity, from 531 to 568 $\text{mPa}\cdot\text{s}$ at a shear rate of 60 s^{-1} . In order to obtain suspensions with comparable viscosities, the viscosity of the pure alginate suspension was also slightly increased by adding a higher amount of sodium alginate: 3.0 wt % (30 g in 970 mL of water) was used for the pure alginate suspension, compared to 3.0% (w/v; 30 g in 1000 mL of water) in the mixed suspension. This resulted in a viscosity value (562 $\text{mPa}\cdot\text{s}$ at a shear rate of 60 s^{-1}) that was comparable with that of the mixed alginate–silica M600 suspension.

Vibrational Droplet Coagulation Process. First of all, the nozzle parameters for the vibrational droplet coagulation procedure were optimized. To visualize the interruption of the laminar jet, a stroboscopic light source was used. When the stroboscope is flashed in phase with the vibrating nozzle, the apparent continuous stream could be detected by the eye as distinct droplets. The instrument parameters were optimized in such a way that (1) droplets were observed at a stable position, instead of oscillating in the stream, which would indicate a labile breakup, and (2) no satellite droplets (smaller droplets between the main droplets) were observed. The latter would indicate that the feed pressure is too high. The influence of the feed pressure on the breakup of the laminar jet is visualized in Figure 4.

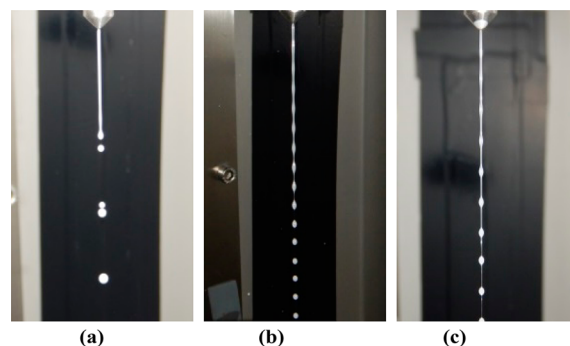


Figure 4. Visualization of the effect of parameter variation on the breakup of the annular jet. Increasing feed pressure from left to right. In part a, the pressure is too low to get a good breakup for a suspension with this viscosity. In part b, a perfect breakup is shown because the right settings were applied here. In part c, the presence of satellite droplets between the main droplets can be observed as a consequence of too high pressure.

Optimization of the parameters highly depends on the composition of the suspension because its characteristics (rheology, surface tension, density, etc.) are related to this. Moreover, the morphology of the produced microspheres will depend on the experimental conditions. For instance, when dripping two suspensions with the exact same composition, higher vibration frequencies will result in smaller spheres. The parameters used for both processes are summarized in Table S2.

Because of the pressure at which suspensions are dripped through the nozzle, the impact between the dripped microspheres and the surface of the coagulation solution is considerable. Nevertheless, it was not necessary to lower the surface tension of the coagulation bath (typically with isopropyl alcohol) in order to maintain the spherical shape. This indicates that the coagulation mechanism was sufficiently strong. It was also observed that a coagulation bath with a CaCl_2

concentration of 2.5% (w/v) resulted in more spherical microspheres compared to a concentration of 5.0% (w/v). This has to do with the speed at which coagulation occurs because a lower salt concentration results in a slower coagulation mechanism. This allows a settling period for the microspheres to regain their initial spherical shape from the oval shape that resulted after the high impact against the coagulation surface. Moreover, a slower coagulation mechanism helps to avoid the enclosure of tiny air bubbles within the microspheres, which would otherwise cause microspheres to float on the surface, therefore hindering and deforming incoming spheres. With a CaCl_2 concentration of 2.5% (w/v), spheres immediately sank to the bottom.

The water content was determined for pure alginate, alginate–TMOS, and alginate–silica M600 microspheres (Table 1). The water content is a measure for the porosity of

Table 1. Values for the Water Content of the Synthesized Microspheres^a

	water content (%)	solid material (%)
pure alginate	96.6	3.4
alginate–TMOS	91.5	8.5
alginate–silica M600	94.0	6.0

^aPercentages of the solid material were calculated from the water content.

the microspheres. In all microspheres, the major part (>90%) consists of pores, which impact the permeability of the microspheres required to ensure a smooth flow when they are applied in a column chromatography setup. In the wet state, the total pore (water) volume is the highest in the pure alginate microspheres. Incorporation of silica increases the amount of solid material and occupation of free pores. The total share of solid material is higher in the alginate–TMOS microspheres, in which silica polymerization reactions were induced in situ, compared to the alginate–silica M600 beads, in which commercial silica powder was dispersed.

FTIR Spectroscopy Analysis. FTIR absorption spectra confirmed the presence of alginate and silica material in both batches (Supporting Information). Characteristic wavenumbers in the pure calcium alginate spheres were localized at 3000–3600 cm^{-1} (broad band, –OH), 1587 cm^{-1} (primary peak carboxylate, shifted from 1595 cm^{-1} compared to the original sodium alginate powder), 1415 cm^{-1} (secondary peak, carboxylate, shifted from 1407 cm^{-1} compared to the original sodium alginate powder), and 1021 cm^{-1} (C–O stretch). These bands also appeared in the hybrid alginate–silica microspheres, except for the band at 1021 cm^{-1} , because of the presence of a more significant intense band at 1063 cm^{-1} (Si–O–Si in alginate–TMOS) or 1034 cm^{-1} (Si–O–Si in alginate–silica M600). Also the broad band between 3000 and 3600 cm^{-1} was less pronounced in the alginate–TMOS particles, just like the band at 1587 cm^{-1} disappeared in the alginate–TMOS spheres. The latter two observations were quite unexpected. It seems that the vibrations of both hydroxyl and carboxylate groups in pure alginate disappeared by reaction with the silanol entities in the formation of an IPN structure. Next, an extra silica peak appeared at 798 cm^{-1} (in alginate–TMOS) and 794 cm^{-1} (in alginate–silica M600), arising from Si–OH vibrations. In the IR spectrum of the alginate–TMOS particles, an additional peak at 958 cm^{-1} (silicate ion) was observed.

Morphology Analysis. The microspheres were investigated by optical microscopy to qualitatively confirm the spherical shape, monomodal size distribution, and micrometer size (Figure 5).



Figure 5. Optical microscopy picture of alginate–silica M600 microspheres. Amplification: 8X.

Quantification of the particle-size distribution was done on a minimum count of 100 microspheres. Results for the wet alginate–TMOS and alginate–silica M600 microspheres are summarized in Table 2. On the one hand, the d_{90}/d_{10} ratio is a

Table 2. Particle-Size Values (Mean Diameter and d_{90}/d_{10} and Mean Feret Ratios) for Wet Alginate–Silica Microspheres

	diameter (μm)	d_{90}/d_{10}	Feret ratio
alginate–TMOS	781 \pm 37	1.12	0.90 \pm 0.04
alginate–silica M600	1100 \pm 17	1.04	0.95 \pm 0.02

measure for the homogeneity of the different particle sizes in the population. The closer this ratio approaches 1, the more uniform the particle-size distribution is. On the other hand, the Feret ratio is a measure for the degree of circularity:

$$\text{Feret ratio} = d/D \quad (4)$$

with d the minimum Feret diameter and D the maximum Feret diameter. A Feret diameter is defined as the distance between two parallel tangential lines of a sphere. A Feret ratio of 1 indicates a perfectly spherical microsphere.

Particle-size measurements revealed smaller microspheres for the batch of alginate–TMOS compared to that for alginate–silica M600. This can be explained by the different compositions of the corresponding suspensions and with experimental conditions, like the vibrational frequency at which the microspheres were dripped: the pure alginate–TMOS microspheres, dripped at a frequency of 750 Hz, are almost 30% smaller than the alginate–silica M600 microspheres, which were dripped at a frequency of 350 Hz. Results also show a tight particle-size distribution for both batches (d_{90}/d_{10} value close to 1) and confirm that the particles can be considered spherical (Feret ratio ≥ 0.90). However, it is also clear that a higher degree of uniformity and circularity was obtained for the alginate–silica M600 microspheres. Besides more deformations, higher standard deviations are observed for the diameters of the alginate–TMOS microspheres. Plausible explanations for this are (1) smaller spheres have less weight and are deformed more upon impact against the surface of the coagulation bath, (2) the faster coagulation of the smaller spheres did not allow for sufficient relaxation, and (3) these

microspheres have endured more physical handling during their synthesis. A combination of these effects is also likely.

A SEM analysis was performed on supercritical CO₂ dried microspheres in order to investigate the surfaces of the microspheres (Figure 6). The microsphere surfaces are well-

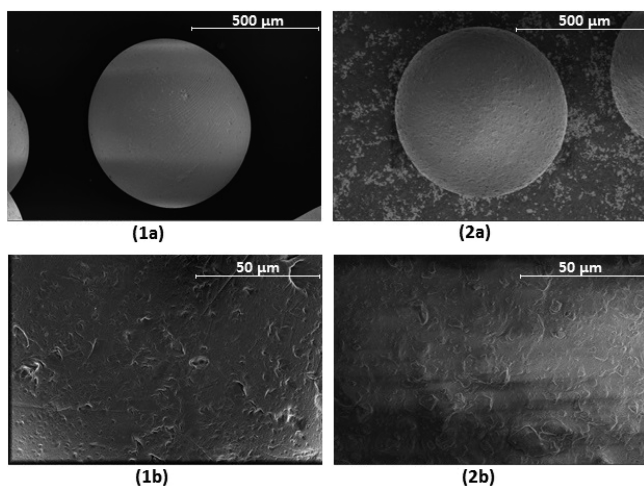


Figure 6. SEM images of the surfaces of alginate–TMOS (1) and alginate–silica M600 (2) microspheres. Images were made at an acceleration voltage of 5.00 kV, a working distance of 6.5 mm, and magnifications of 100× (a) and 1000× (b).

defined. A smoother surface is observed for the alginate–TMOS microspheres. The alginate–silica M600 microspheres are characterized by a coarser surface with small local elevations.

Specific Surface Area. A BET analysis was performed on freeze-dried microspheres to measure the specific surface area of the materials. For the alginate–TMOS microspheres, the specific surface area corresponded to 216.1 m²/g, a significantly higher value than the one obtained for the alginate–silica M600 microspheres with a specific surface area of 4.6 m²/g. The latter, low value was predicted from the specifications of the added silica powder. Sikron M600 has a specific surface area of 4.2 m²/g as determined by the producer. The alginate material did not contribute to an increase of the total specific surface area. A composite alginate–silica material with a higher total specific surface area could be obtained by using a silica powder that is characterized by an intrinsically higher specific surface area. However, this could cause problems in the process because it will also lead to higher viscosity values for the suspensions to be dripped. On the other side, the pure alginate microspheres that were soaked in a TMOS solution afterward showed a high specific surface area. This can be attributed to the in situ polymerization of silica networks. A high specific surface area guarantees a good availability of the functional groups.

Comparison of Different Drying Methods. Storage of microspheres is easier when they are dried. However, drying causes damage to the raw porous structure of the alginate–silica microspheres. This has to do with capillary forces that result from the surface tension of water when going from the liquid to the gaseous phase. Special drying procedures, like freeze-drying and supercritical CO₂ drying, avoid crossing the liquid–gas phase boundary and therefore prevent collapse of the raw structure. With freeze-drying, microspheres are frozen with liquid nitrogen and then put under a vacuum, so that frozen

water can be sublimated. With supercritical CO₂ drying, the pressure and temperature are increased in a chamber containing wet microspheres soaked in liquid CO₂. In this way, it is possible to pass the critical point of CO₂ (73.8 bar and 31 °C) at which the fluid becomes neither liquid nor gas. Supercritical CO₂ can then be released, leaving behind the dried sample.

By means of optical microscopy, a particle-size analysis was performed for the differently dried microspheres. The amount of shrinkage was compared. The shrink percentage is defined as

$$\text{shrink percentage} = \frac{D_{\text{wet}} - D_{\text{dry}}}{D_{\text{wet}}} \times 100\% \quad (5)$$

with D_{wet} the mean diameter of the wet microspheres (before drying) and D_{dry} the mean diameter of the dry microspheres (after drying). The closer the shrink percentage approaches 0%, the less shrinkage has occurred. The shrinkage data for both materials dried to the air, by freeze-drying and by supercritical CO₂ drying, are summarized in Table S3.

The most pronounced shrinkage (size and shape) was observed for the microspheres that were dried to the air, which was expected because no care was taken to control the drying process. Moreover, a remarkable difference was observed between both batches. The air-dried alginate–TMOS spheres shrunk only half as much as the alginate–silica M600 spheres. Apparently, the original porous structure of alginate–TMOS microspheres remains much more intact after drying by the formation of a hybrid material with IPNs instead of creating a composite material. With the freeze-drying technique, we seemingly face the limits of the alginate structure to resist shrinkage. In both alginate–silica batches, the microspheres shrank about 23–24%. Moreover, cracks occurred in the freeze-dried microspheres as a consequence of the liquid-nitrogen freezing step. As a result, part of the particles lost their original spherical shape, which explains the lower Feret ratios that resulted from the freeze-drying technique, even lower than those for microspheres that were dried to the air. With supercritical CO₂ drying, crack formation can be avoided because there is no freezing step. There is also no need for extremely high temperatures or vacuum conditions, so that the technique is generally considered more controlled and also more energy-efficient than conventional drying techniques. A shrink percentage of 24% was again observed for the alginate–silica M600 particles that were dried by supercritical CO₂, but a better value was obtained for the alginate–TMOS microspheres. Here, the effect of creating IPNs by soaking with TMOS clearly appears. The latter leads to a more rigid, supporting matrix structure, which, in combination with the supercritical CO₂ drying technique, leads to the best preserved structure in the dry state. Depending on the final application, it is more interesting to add dispersed silica powder rather than to induce silica polymerization afterward. In the alginate–TMOS spheres, the porous structure is better stabilized and a material with a significantly higher specific surface area is obtained. In the alginate–silica M600 composite materials, the silica powder merely serves as a filling material. In the hydrometallurgical applications that are the target of this work, the spheres are used in a wet state. The shrinkage induced by drying is therefore less relevant compared to the different sources of silica, which impact the adsorption and column performance. The ease of adding dispersible silica powder with known and proper characteristics to an alginate suspension could be a more decisive factor, unless one wants to incorporate specific

functional groups. Then it would be interesting to induce the silica polymerization reactions starting from, for instance, functionalized siloxanes.

It is further important to mention that the shrinkage by drying seemed to be irreversible. The swelling behavior was investigated for both batches that were dried either way. It appeared that the particles did not reswell significantly (>1%) by soaking the microspheres in water for 24 h. This indicates that the collapse of the raw porous structure during drying is not reversible.

Composition. The organic and inorganic share in the alginate–silica hybrid microspheres was determined by combining information derived from both CHN elemental analysis and TGA (Table 3). Air-dried spheres were used for both analyses.

Table 3. CHN Analysis and TGA Results for Different Materials and Corresponding Calculated Values for the Organic Content

	C/H/N (wt %)	organic content calculated from CHN (wt %)	residual mass (TGA) (wt %)	organic content calculated from TGA (wt %)
pure (calcium) alginate	32.5/4.7/0.0	100.0	14.0	100.0
alginate–TMOS	8.1/1.9/0.0	26.0	72.5	31.1
alginate–silica M600	13.6/3.2/0.0	43.7	60.9	45.2

Although calcium(II) (Ca^{II}) is built in the alginate structure, it is considered here as part of the organic share in the hybrid microspheres. In this way, it is possible to estimate the organic content in the hybrid alginate–silica microspheres by a comparison of the carbon percentages in the hybrid alginate–silica microspheres with the percentages in pure (calcium) alginate microspheres.

TGA was used as a supplementary technique to confirm the results obtained by CHN analysis (Figure S3). Residual masses arise from the silica content intrinsically present in the microspheres and from CaCO_3 formed during heating by the reaction of coagulated calcium ions with O_2 in the air.⁵⁵ The amount of coagulated Ca^{II} ions in the microspherical alginate structures could be calculated from the TGA trace of pure (calcium) alginate and the organic share in the hybrid microspheres, derived from CHN analysis.

From the results obtained by CHN analysis and TGA, it can be concluded that the amount of inorganic silica material is significantly higher in the alginate–TMOS microspheres, compared to the alginate–silica M600 microspheres. This is a consequence of the less controllable procedure that was followed to incorporate silica in the alginate–TMOS microspheres. When in situ silica polymerization reactions were induced, higher amounts of inorganic silica were obtained in these hybrid materials. Because the amount of organic (functional) material is lower in the alginate–TMOS microspheres, it can be expected that the adsorption capacity will also be lower for these microspheres (vide infra).

Stability as a Function of the pH. Wet microspheres were stirred in solutions with increasing concentrations of HCl. In none of the particles was loss of silicon detected by TXRF. The release of Ca^{2+} ions is presented in Figure S4. For pure alginate

microspheres, the calcium release appeared to gradually increase with higher HCl concentrations. In the hybrid microspheres (both alginate–TMOS and alginate–silica M600), the release of calcium ions was lower at low HCl concentrations and also increased less significantly with higher HCl concentrations. The slightly higher release of Ca^{II} from the alginate–TMOS microspheres, compared to the alginate–silica M600 microspheres, can be attributed to the fact that the absolute concentration of sodium alginate was slightly higher in the original suspension of sodium alginate [3.0 wt % vs 3.0% (w/v), respectively]. The way in which silica was incorporated did not seem to have an influence on the retention of coagulated Ca^{II} ions.

Adsorption Performance. Because these functional microspheres are intended for hydrometallurgical applications, they must meet some specific requirements. It was already mentioned that the droplet coagulation technology should be feasible to produce high-performance microspheres on a large industrial scale. The convenient microspheres can be used as ion-exchange resin materials in large column setups. Furthermore, it is important that the microspheres have a high adsorption capacity, with affinity for the metal ions of interest. They should also be reusable during consecutive adsorption/desorption cycles without loss of efficiency.

Adsorption was studied for Nd^{III} as a model element for the rare-earth ions. It was reported before that alginate is able to coordinate rare-earth ions thanks to the presence of carboxylic acid functional groups on the alginate moieties.⁴⁰ The uptake of Nd^{III} was investigated as a function of the equilibrium pH for alginate–TMOS and alginate–silica M600 microspheres (Figure 7). Also, the influence of drying on the adsorption amount was investigated.

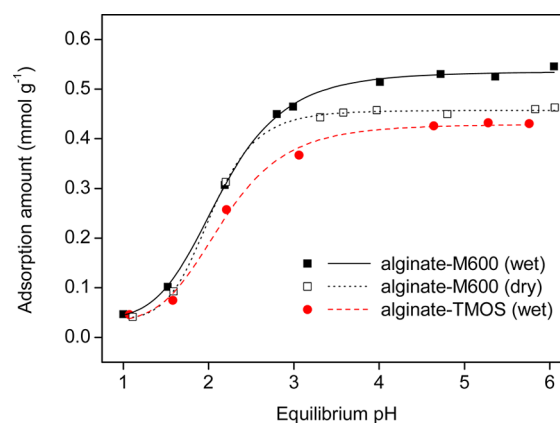


Figure 7. Adsorption of Nd^{III} ions from an aqueous solution by alginate–silica microspheres as a function of the pH. $c(\text{Nd}^{3+}) = 2.00 \pm 0.02$ mM; volume = 10.0 mL; contact time = 4 h; mass adsorbent = 500 ± 5 mg. The adsorption values for the wet spheres were corrected to dry functional mass.

The curves showing the adsorption amount as a function of increasing pH values (Figure 7) have a typical sigmoidal shape because of deprotonation of the functional carboxylic acid groups upon going to higher pH values. At pH = 1, there is hardly any affinity for the Nd^{III} ions present in solution. At a pH of approximately 5–6, maximum adsorption is obtained. Note that, at this concentration, precipitation of Nd^{III} only occurs at pH > 6. The wet alginate–silica M600 microspheres showed the highest absolute adsorption amount for Nd^{III} . The

most probable explanation for this is that the share of organic (functional) material is higher in these microspheres, compared to the alginate–TMOS microspheres. In the alginate–TMOS microspheres, a higher mass ratio consists of a silica matrix material. However, taking into account the share of functional alginate material, the relative adsorption amount for Nd^{III} is higher for the alginate–TMOS microspheres. This is probably attributed to the higher specific surface area of these microspheres: $216.1 \text{ m}^2/\text{g}$ for alginate–TMOS, compared to $4.6 \text{ m}^2/\text{g}$ for alginate–silica M600 (vide supra). A higher specific surface area results in an improved accessibility of the available functional groups. It is interesting to observe how the incorporation of silica can alter the adsorption performance of the hybrid microspheres. It is also observed that the (air-)dried alginate–silica M600 microspheres showed a lower adsorption amount for Nd^{III} compared to the microspheres that were kept in the wet state. Because the microspheres shrank during the drying process, the porosity also lowered. It can therefore be concluded that, besides resulting in an improved eluent flow through a column, the high porosity in the wet microspheres also results in an improved adsorption capacity by a higher availability of the functional groups in these particles, thus facilitating the chelation mechanism. It is also important to mention that the adsorption capacities obtained with these alginate–silica microspheres were higher than the ones obtained in earlier work on ethylenediaminetetraacetic acid (EDTA)- and diethylenetriaminepentaacetic acid (DTPA)-functionalized chitosan–silica powder.⁴⁴ Chitosan is a biopolymer with very similar characteristics compared to alginate. However, while chitosan powder had to be functionalized with the metal-chelating ligands EDTA and DTPA to improve its adsorption capacity, we now observe even higher adsorption capacities with the alginate–silica microspheres, which intrinsically bear carboxylic acid functional groups in their structure: $0.4\text{--}0.5$ vs 0.2 mmol of Nd^{III} per gram of adsorbent, respectively, under similar experimental conditions and a comparable share of functional organic material in the total hybrid sorbents. Next to that, Wang et al. (2013) reported separation coefficients between Nd^{III} and other metal ions for similar alginate adsorbents, following the order $\text{Fe}^{\text{III}} > \text{Nd}^{\text{III}} > \text{Al}^{\text{III}} > \text{Cr}^{\text{III}} > \text{Cu}^{\text{II}} > \text{V}^{\text{V}} > \text{Ni}^{\text{II}} > \text{Co}^{\text{II}} > \text{Mn}^{\text{II}} \gg \text{Cr}^{\text{VI}}$.⁴⁰ On the basis of all of these results, we strongly believe in the application potential of these kinds of microspheres to recover minor amounts of valuable metals (like the rare earths) from waste streams and to separate them from other metal ions with a lower affinity.

Stripping and Reusability. After adsorption of metal ions from solution, stripping of immobilized ions is required for further processing and regeneration of the adsorbent. This was done by bringing the loaded particles in contact with acidified solutions. The microspheres were first loaded by adsorption from an aqueous Nd^{III} solution. The effect of the HCl concentration on the amount of stripping is shown for alginate–TMOS and alginate–silica M600 microspheres in Figure S5. The stripping proceeded easily. No concentrated acid or complex chelating solutions were necessary to desorb the loaded metal ions from the sorbents. Full stripping of immobilized Nd^{III} ions was already observed with a HCl concentration of 0.25 M . This was expected because this concentration equals a pH of about 0.56 , which is lower than 1.00 (at which pH, the affinity for Nd^{III} was negligible). However, it was beneficial that full stripping was obtained with mildly acidic solutions because harsh conditions would

probably have an influence on the adsorption performance of the particles.

The reusability was investigated for the alginate–silica M600 microspheres. A certain amount was subjected to seven consecutive adsorption/desorption cycles, and the resulting adsorption value was compared with the original adsorption amount to determine the adsorption efficiency (Figure 8).

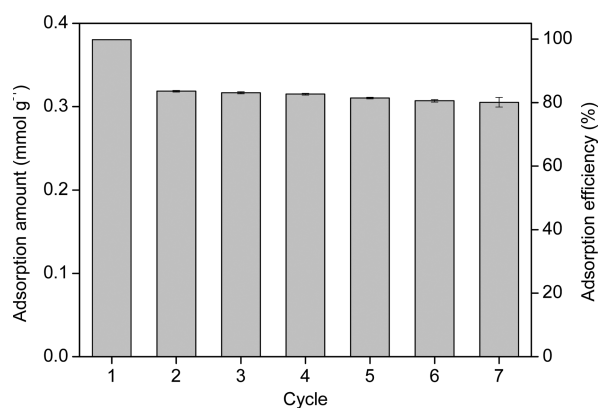


Figure 8. Evolution of the adsorption efficiency of alginate–silica M600 microspheres for consecutive adsorption/desorption cycles of Nd^{III} . All parameters were the same in each cycle. $c(\text{Nd}^{\text{III}}) = 1.00 \pm 0.01 \text{ mM}$; volume = 10.0 mL ; $\text{pH}_{\text{in}} = 4.0$; contact time = 4 h ; mass adsorbent = $500 \pm 5 \text{ mg}$; stripping solution = 0.5 M HCl (10.0 mL); stripping time = 1 h .

The adsorption efficiency decreased by almost 20% in the second adsorption cycle. This is probably due to conformational changes by the acidic attack during the first stripping step. Because the overall coagulation structure of the microspheres remained intact during consecutive stripping steps, the calcium ions tightly held by egg-box interactions between alginate G blocks did apparently not experience any damage from the stripping. However, we believe that the weak junctions in MG blocks were destroyed by replacing the Ca^{II} ions with protons.⁵² As a consequence, the “preorientation” of certain functional groups, induced by the coordination of Ca^{II} from the coagulation bath, is lost, and as a result, coordination of Nd^{III} becomes less favorable. The residual capacity remained quite constant. In none of the subsequent cycles was further significant loss in the adsorption efficiency observed, which can be explained by the fact that all weakly stabilized conformations were already destroyed in the first stripping step. These findings were supported by the observation of Ca^{II} release during the first stripping step but no longer during consequent stripping steps. After the seventh adsorption cycle, the adsorption efficiency is still higher than 80%. Moreover, the observed (minimal) decrease after the second cycle could more likely be attributed to physical losses because of the manual handlings during consecutive adsorption/desorption cycles rather than to physical or chemical damage to the particles because of the stripping treatment. It is therefore suggested to include an acidic treatment of the microspheres as a last step in the synthesis procedure, in order to wash out Ca^{II} ions that were adsorbed from the coagulation solution. In this way, the occurrence of specific conformations that could prefer coordination of certain metal ions only in the first cycle will be avoided, and as a consequence, the adsorption efficiency will hardly be affected over time. Hence, the functional microspheres can be considered to be sustainable materials.

CONCLUSIONS

By making use of vibrating-nozzle technology, high-performance microspheres were made by droplet coagulation of a sodium alginate suspension in a solution of CaCl_2 . The synthesis is straightforward and easily convertible to industrial scale thanks to the design of the Microspherisator device. Silica was incorporated (1) by soaking pure alginate microspheres in a TMOS solution to induce in situ silica polymerization reactions and (2) by adding silica powder to the alginate suspension prior to coagulation. The addition of a silica powder to the alginate suspension benefits from its easy, one-step synthesis and the fact that the characteristics of the resulting material are highly predictable, arising from the characteristics of the added silica source. On the other hand, the formation of an IPN material results in a material with a good resistance to shrinkage during drying, a high stability in an acidic environment and a high specific surface area. The latter leads to a better availability of the functional groups. Moreover, by using functionalized siloxanes, any functional group could be built in the microspheres in this way, depending on the metal of interest. The carboxylic acid functional groups intrinsically present on the alginate chains show a high affinity for hard ions like the REEs, of which neodymium was considered in this work. However, other metals, like the platinum group metals, would benefit from an organic ligand with a soft character. The microspheres of alginate–silica M600 composite and alginate–TMOS IPN materials were fully characterized regarding their morphology and composition. Regarding their use in hydro-metallurgical applications, the microspheres were proven to be stable in a very broad acidity range. The adsorption amount of Nd^{III} reached 0.43 mmol/g for alginate–TMOS microspheres and 0.46 mmol/g for alginate–silica M600 microspheres. Stripping of loaded microspheres could be achieved with a simple inorganic acid, like hydrochloric acid. A concentration of 0.25 M was already sufficient to get 100% stripping. The microspheres are considered to be sustainable materials because the adsorption efficiency remained constant during consecutive adsorption/desorption cycles, apart from a drop after the first desorption cycle.

ASSOCIATED CONTENT

Supporting Information

The Supporting Information is available free of charge on the ACS Publications website at DOI: 10.1021/acs.iecr.5b03494.

Ostwald–de Waele model fitting parameters for suspension viscosities, experimental parameters for vibrational droplet coagulation experiments, FTIR spectra, shrinkage data resulting from different drying techniques, TGA traces, Ca^{II} release as a function of the HCl concentration, and stripping percentage as a function of the HCl concentration (PDF)

AUTHOR INFORMATION

Corresponding Author

*E-mail: Koen.Binnemans@chem.kuleuven.be. Tel: +32 16 32 7446.

Author Contributions

The manuscript was written through contributions of all authors. All authors have given approval to the final version of the manuscript.

Notes

The authors declare no competing financial interest.

ACKNOWLEDGMENTS

The authors thank VITO, the Research Foundation—Flanders (FWO Ph.D. fellowship to J.R.), and KU Leuven (Projects GOA 13/008 and IOF-KP RARE³) for the funding of this research. Bart Michiels is acknowledged for his help and advice with the vibrational droplet coagulation experiments. The technical staff is acknowledged for carrying out most of the analyses: Annemie De Wilde (TGA and BET), Raymond Kemps (SEM), and Jef De Wit (CHN).

REFERENCES

- (1) Fomina, M.; Gadd, G. M. Biosorption: current perspectives on concept, definition and application. *Bioresour. Technol.* **2014**, *160*, 3–14.
- (2) Wang, J.; Chen, C. Chitosan-based biosorbents: modification and application for biosorption of heavy metals and radionuclides. *Bioresour. Technol.* **2014**, *160*, 129–141.
- (3) Won, S. W.; Kotte, P.; Wei, W.; Lim, A.; Yun, Y. S. Biosorbents for recovery of precious metals. *Bioresour. Technol.* **2014**, *160*, 203–212.
- (4) Babel, S.; Kurniawan, T. A. Low-cost adsorbents for heavy metals uptake from contaminated water: a review. *J. Hazard. Mater.* **2003**, *97*, 219–243.
- (5) Chang, Y.-H.; Huang, C.-F.; Hsu, W.-J.; Chang, F.-C. Removal of Hg^{2+} from aqueous solution using alginate gel containing chitosan. *J. Appl. Polym. Sci.* **2007**, *104*, 2896–2905.
- (6) Gerente, C.; Lee, V. K. C.; Cloirec, P. L.; McKay, G. Application of Chitosan for the Removal of Metals From Wastewaters by Adsorption—Mechanisms and Models Review. *Crit. Rev. Environ. Sci. Technol.* **2007**, *37*, 41–127.
- (7) Wang, J.; Chen, C. Biosorbents for heavy metals removal and their future. *Biotechnol. Adv.* **2009**, *27*, 195–226.
- (8) Vijaya, Y.; Popuri, S. R.; Boddu, V. M.; Krishnaiah, A. Modified chitosan and calcium alginate biopolymer sorbents for removal of nickel (II) through adsorption. *Carbohydr. Polym.* **2008**, *72*, 261–271.
- (9) Guibal, E. Interactions of metal ions with chitosan-based sorbents: a review. *Sep. Purif. Technol.* **2004**, *38*, 43–74.
- (10) Crini, G. Non-conventional low-cost adsorbents for dye removal: a review. *Bioresour. Technol.* **2006**, *97*, 1061–85.
- (11) Coradin, T.; Nassif, N.; Livage, J. Silica-alginate composites for microencapsulation. *Appl. Microbiol. Biotechnol.* **2003**, *61*, 429–434.
- (12) Hoffmann, F.; Cornelius, M.; Morell, J.; Froba, M. Silica-based mesoporous organic-inorganic hybrid materials. *Angew. Chem., Int. Ed.* **2006**, *45*, 3216–3251.
- (13) Lan, W.; Li, S.; Xu, J.; Luo, G. One-step synthesis of chitosan-silica hybrid microspheres in a microfluidic device. *Biomed. Microdevices* **2010**, *12*, 1087–1095.
- (14) Molvinger, K.; Quignard, F.; Brunel, D.; Boissiere, M.; Devoisselle, J.-M. Porous Chitosan-Silica Hybrid Microspheres as a Potential Catalyst. *Chem. Mater.* **2004**, *16*, 3367–3372.
- (15) Pandis, C.; Madeira, S.; Matos, J.; Kyritsis, A.; Mano, J. F.; Ribelles, J. L. G. Chitosan–silica hybrid porous membranes. *Mater. Sci. Eng., C* **2014**, *42*, 553–561.
- (16) Rashidova, S. S.; Shakarova, D. S.; Ruzimuradov, O. N.; Satubaldieva, D. T.; Zalyalieva, S. V.; Shpigun, O. A.; Varlamov, V. P.; Kabulov, B. D. Bionanocompositional chitosan-silica sorbent for liquid chromatography. *J. Chromatogr. B: Anal. Technol. Biomed. Life Sci.* **2004**, *800*, 49–53.
- (17) Smitha, S.; Shajesh, P.; Mukundan, P.; Warriar, K. G. K. Sol-gel synthesis of biocompatible silica-chitosan hybrids and hydrophobic coatings. *J. Mater. Res.* **2008**, *23*, 2053–2060.
- (18) Walcarius, A.; Mercier, L. Mesoporous organosilica adsorbents: nanoengineered materials for removal of organic and inorganic pollutants. *J. Mater. Chem.* **2010**, *20*, 4478–4511.

- (19) Wu, C.; Fan, W.; Gelinsky, M.; Xiao, Y.; Chang, J.; Friis, T.; Cuniberti, G. In situ preparation and protein delivery of silicate-alginate composite microspheres with core-shell structure. *J. R. Soc., Interface* **2011**, *8*, 1804–1814.
- (20) Whelehan, M.; Marison, I. W. Microencapsulation using vibrating technology. *J. Microencapsulation* **2011**, *28*, 669–688.
- (21) Thies, C. Microcapsules. In *Encyclopedia of Food Sciences and Nutrition*, 2nd ed.; Caballero, B., Ed.; Academic Press: Oxford, U.K., 2003; pp 3892–3903.
- (22) Sri, J.; Seethadevi, A.; Prabha, K. S.; Muthuprasanna, P.; Pavitra, P. Microencapsulation: a review. *Int. J. Pharm. Biol. Sci.* **2012**, *13*, 509–531.
- (23) Lam, P. L.; Gambari, R. Advanced progress of microencapsulation technologies: In vivo and in vitro models for studying oral and transdermal drug deliveries. *J. Controlled Release* **2014**, *178*, 25–45.
- (24) Ma, G. Microencapsulation of protein drugs for drug delivery: Strategy, preparation, and applications. *J. Controlled Release* **2014**, *193*, 324–340.
- (25) Cook, M. T.; Tzortzis, G.; Charalampopoulos, D.; Khutoryanskiy, V. V. Microencapsulation of probiotics for gastrointestinal delivery. *J. Controlled Release* **2012**, *162*, 56–67.
- (26) Nesterenko, A.; Alric, I.; Silvestre, F.; Durrieu, V. Vegetable proteins in microencapsulation: A review of recent interventions and their effectiveness. *Ind. Crops Prod.* **2013**, *42*, 469–479.
- (27) Martin, M. J.; Lara-Villoslada, F.; Ruiz, M. A.; Morales, M. E. Microencapsulation of bacteria: A review of different technologies and their impact on the probiotic effects. *Innovative Food Sci. Emerging Technol.* **2015**, *27*, 15–25.
- (28) Sobel, R.; Versic, R.; Gaonkar, A. G. Introduction to Microencapsulation and Controlled Delivery in Foods. In *Microencapsulation in the Food Industry*; Gaonkar, A. G., Vasisht, N., Khare, A. R., Sobel, R., Eds.; Academic Press: San Diego, CA, 2014; Chapter 1, pp 3–12.
- (29) Li, F.; Li, X.-M.; Zhang, S.-S. One-pot preparation of silica-supported hybrid immobilized metal affinity adsorbent with macroporous surface based on surface imprinting coating technique combined with polysaccharide incorporated sol-gel process. *J. Chromatogr. A* **2006**, *1129*, 223–230.
- (30) Jacobs, I. C. Atomization and Spray-Drying Processes. In *Microencapsulation in the Food Industry*; Gaonkar, A. G., Vasisht, N., Khare, A. R., Sobel, R., Eds.; Academic Press: San Diego, CA, 2014; Chapter 5, pp 47–56.
- (31) Frey, C., Fluid Bed Coating-Based Microencapsulation. In *Microencapsulation in the Food Industry*; Gaonkar, A. G., Vasisht, N., Khare, A. R., Sobel, R., Eds.; Academic Press: San Diego, CA, 2014; Chapter 7, pp 65–79.
- (32) Yan, C.; Zhang, W. Coacervation Processes. In *Microencapsulation in the Food Industry*; Gaonkar, A. G., Vasisht, N., Khare, A. R., Sobel, R., Eds.; Academic Press: San Diego, CA, 2014; Chapter 12, pp 125–137.
- (33) Jacob, M. Spheronization, Granulation, Pelletization, and Agglomeration Processes. In *Microencapsulation in the Food Industry*; Gaonkar, A. G., Vasisht, N., Khare, A. R., Sobel, R., Eds.; Academic Press: San Diego, CA, 2014; Chapter 9, pp 85–98.
- (34) Brandau, T. Annular Jet-Based Processes. In *Microencapsulation in the Food Industry*; Gaonkar, A. G., Vasisht, N., Khare, A. R., Sobel, R., Eds.; Academic Press: San Diego, CA, 2014; Chapter 10, pp 99–110.
- (35) Heichal-Segal, O.; Rappoport, S.; Braun, S. Immobilization in Alginate-Silicate Sol-Gel Matrix Protects β -Glucosidase Against Thermal and Chemical Denaturation. *Bio/Technology* **1995**, *13*, 798–800.
- (36) Brinker, C. F.; Scherer, G. W. *Sol-Gel Science. The Physics and Chemistry of Sol-Gel Processing*; Academic Press: San Diego, CA, 1990; p 908.
- (37) Binnemans, K.; Jones, P. T.; Blanpain, B.; Van Gerven, T.; Pontikes, Y. Towards zero-waste valorisation of rare-earth-containing industrial process residues: a critical review. *J. Cleaner Prod.* **2015**, *99*, 17–38.
- (38) Gotoh, T.; Matsushima, K.; Kikuchi, K.-I. Preparation of alginate-chitosan hybrid gel beads and adsorption of divalent metal ions. *Chemosphere* **2004**, *55*, 135–140.
- (39) Ngah, W. S. W.; Fatinathan, S. Adsorption of Cu(II) ions in aqueous solution using chitosan beads, chitosan-GLA beads and chitosan-alginate beads. *Chem. Eng. J.* **2008**, *143*, 62–72.
- (40) Wang, F.; Zhao, J.; Pan, F.; Zhou, H.; Yang, X.; Li, W.; Liu, H. Adsorption Properties toward Trivalent Rare Earths by Alginate Beads Doping with Silica. *Ind. Eng. Chem. Res.* **2013**, *52*, 3453–3461.
- (41) Wang, F.; Zhao, J.; Wei, X.; Huo, F.; Li, W.; Hu, Q.; Liu, H. Adsorption of rare earths (III) by calcium alginate-poly glutamic acid hybrid gels. *J. Chem. Technol. Biotechnol.* **2014**, *89*, 969–977.
- (42) Wang, F. C.; Zhao, J. M.; Liu, H. Z. Adsorption of Nd(III) by silicate-alginate composite beads containing 2-ethylhexyl phosphonic acid mono-2-ethylhexyl ester. *Rare Earths* **2012**, Niagara, Ontario, Canada, 2012; Goode, J. R., Moldoveanu, G., Rayat, M. S., Eds.; Avalon Metals Inc.: Toronto, Ontario, Canada, 2012; pp 261–267.
- (43) Roosen, J.; Binnemans, K. Adsorption and chromatographic separation of rare earths with EDTA- and DTPA-functionalized chitosan biopolymers. *J. Mater. Chem. A* **2014**, *2*, 1530–1540.
- (44) Roosen, J.; Spooren, J.; Binnemans, K. Adsorption performance of functionalized chitosan-silica hybrid materials toward rare earths. *J. Mater. Chem. A* **2014**, *2*, 19415–19426.
- (45) Estevinho, B. N.; Rocha, F.; Santos, L.; Alves, A. Microencapsulation with chitosan by spray drying for industry applications – A review. *Trends Food Sci. Technol.* **2013**, *31*, 138–155.
- (46) El Kadib, A.; Bousmina, M. Chitosan bio-based organic-inorganic hybrid aerogel microspheres. *Chem. - Eur. J.* **2012**, *18*, 8264–8277.
- (47) Vitali, L.; Laranjeira, M. C.; Goncalves, N. S.; Favere, V. T. Spray-dried chitosan microspheres containing 8-hydroxyquinoline –5 sulphonic acid as a new adsorbent for Cd(II) and Zn(II) ions. *Int. J. Biol. Macromol.* **2008**, *42*, 152–157.
- (48) Vu, D.; Li, X.; Wang, C. Adsorption of As(III) from aqueous solution based on porous magnetic/chitosan/ferric hydroxide microspheres prepared via electrospraying. *Sci. China: Chem.* **2013**, *56*, 678–684.
- (49) Zhao, H.; Xu, J.; Lan, W.; Wang, T.; Luo, G. Microfluidic production of porous chitosan/silica hybrid microspheres and its Cu(II) adsorption performance. *Chem. Eng. J.* **2013**, *229*, 82–89.
- (50) Zhao, L.; Zhang, Z. Mechanical characterization of biocompatible microspheres and microcapsules by direct compression. *Artif. Cell. Blood Substit. Biotechnol.* **2004**, *32*, 25–40.
- (51) Guibal, E.; Vincent, T.; Blondet, F. P. *Ion Exchange and Solvent Extraction: A Series of Advances*. In Sen Gupta, A. K., Ed.; CRC Press: Boca Raton, FL, 2007; Vol. 18, pp 151–292.10.1201/9781420007411.ch4
- (52) Pawar, S. N.; Edgar, K. J. Alginate derivatization: a review of chemistry, properties and applications. *Biomaterials* **2012**, *33*, 3279–305.
- (53) Chhabra, R. P.; Richardson, J. F. *Non-Newtonian Flow and Applied Rheology: Engineering Applications*, 2nd ed.; Elsevier: Oxford, U.K., 2008; p 536.
- (54) Belton, D. J.; Deschaume, O.; Perry, C. C. An overview of the fundamentals of the chemistry of silica with relevance to biosilicification and technological advances. *FEBS J.* **2012**, *279*, 1710–1720.
- (55) Konga, Q.-S.; Wang, B. B.; Ji, Q.; Xia, Y.-Z.; Guo, Z.-X.; Yu, J. Thermal degradation and flame retardancy of calcium alginate fibers. *Chin. J. Polym. Sci.* **2009**, *27*, 807–812.